View metadata, citation and similar papers at core.ac.uk
brought to you by CORE
provided by National Chung Hsing University Institutional Repository

Pulsed laser deposition of hexagonal GaN-on-Si(100) template for MOCVD applications

Kun-Ching Shen,[1] Ming-Chien Jiang,[1] Hong-Ru Liu,[1] Hsu-Hung Hsueh,[2] Yu-Cheng Kao,[2] Ray-Hua Horng,[2] and Dong-Sing Wuu[1,3,4,*]

[1] *Department of Materials Science and Engineering, National Chung Hsing University, Taichung 40227, Taiwan*
[2] *Graduate Institute of Precision Engineering, National Chung Hsing University, Taichung 40227, Taiwan*
[3] *Department of Materials Science and Engineering, Da-Yeh University, Changhua 51591, Taiwan*
[4] *Advanced Optoelectronic Technology Center, National Cheng Kung University, Tainan 70101, Taiwan*
**dsw@nchu.edu.tw*

Abstract: Growth of hexagonal GaN on Si(100) templates via pulsed laser deposition (PLD) was investigated for the further development of GaN-on-Si technology. The evolution of the GaN growth mechanism at various growth times was monitored by SEM and TEM, which indicated that the GaN growth mode changes gradually from island growth to layer growth as the growth time increases up to 2 hours. Moreover, the high-temperature operation (1000°C) of the PLD meant no significant GaN meltback occurred on the GaN template surface. The completed GaN templates were subjected to MOCVD treatment to regrow a GaN layer. The results of X-ray diffraction analysis and photoluminescence measurements show not only the reliability of the GaN template, but also the promise of the PLD technique for the development of GaN-on-Si technology.

©2013 Optical Society of America

OCIS codes: (160.2100) Electro-optical materials; (160.6000) Semiconductor materials.

References and links

1. C. Mo, W. Fang, Y. Pu, H. Liu, and F. Jiang, "Growth and characterization of InGaN blue LED structure on Si(111) by MOCVD," J. Cryst. Growth **285**(3), 312–317 (2005).
2. J. Liu, F. Feng, Y. Zhou, J. Zhang, and F. Jiang, "Stability of Al/Ti/Au contacts to N-polar n-GaN of GaN based vertical light emitting diode on silicon substrate," Appl. Phys. Lett. **99**(11), 111112 (2011).
3. A. Dadgar, C. Hums, A. Diez, J. Blasing, and A. Krost, "Growth of blue GaN LED structures on 150-mm Si(111)," J. Cryst. Growth **297**(2), 279–282 (2006).
4. S. Tripathy, V. K. X. Lin, S. B. Dolmanan, J. P. Y. Tan, R. S. Kajen, L. K. Bera, S. L. Teo, M. K. Kumar, S. Arulkumaran, G. I. Ng, S. Vicknesh, S. Todd, W. Z. Wang, G. Q. Lo, H. Li, D. Lee, and S. Han, "AlGaN/GaN two-dimensional-electron gas heterostructures on 200 mm diameter Si(111)," Appl. Phys. Lett. **101**(8), 082110 (2012).
5. K. Radhakrishnan, N. Dharmarasu, Z. Sun, S. Arulkumaran, and G. I. Ng, "Demonstration of AlGaN/GaN high-electron-mobility transistors on 100 mm diameter Si(111) by plasma-assisted molecular beam epitaxy," Appl. Phys. Lett. **97**(23), 232107 (2010).
6. W. E. Fenwick, A. Melton, T. Xu, N. Li, C. Summers, M. Jamil, and I. T. Ferguson, "Metal organic chemical vapor deposition of crack-free GaN-based light emitting diodes on Si(111) using a thin Al_2O_3 interlayer," Appl. Phys. Lett. **94**(22), 222105 (2009).
7. A. Watanabe, T. Takeuchi, K. Hirosawa, H. Amano, K. Hiramatsu, and I. Akasaki, "The growth of single crystalline GaN on a Si substrate using AlN as an intermediate layer," J. Cryst. Growth **128**(1–4), 391–396 (1993).
8. K. L. Lin, E. Y. Chang, Y. L. Hsiao, W. C. Huang, T. Li, D. Tweet, J. S. Maa, S. T. Hsu, and C. T. Lee, "Growth of GaN film on 150 nm Si (111) using multilayer AlN/AlGaN buffer by metal-organic vapor phase epitaxy method," Appl. Phys. Lett. **91**(22), 222111 (2007).
9. Y. Nakada, I. Aksenov, and H. Okumura, "GaN heteroepitaxial growth on silicon nitride buffer layers formed on Si(111) surfaces by plasma-assisted molecular beam epitaxy," Appl. Phys. Lett. **73**(6), 827–829 (1998).
10. D. Deng, N. Yu, Y. Wang, X. Zou, H. C. Kuo, P. Chen, and K. M. Lau, "InGaN-based light-emitting diodes grown and fabricated on nanopatterned Si substrates," Appl. Phys. Lett. **96**(20), 201106 (2010).

11. J. T. Ku, T. H. Yang, J. R. Chang, Y. Y. Wong, W. C. Chou, C. Y. Chang, and C. Y. Chen, "Epitaxial overgrowth of gallium nitride nano-rods on silicon (111) substrates by RF-plasma-assisted molecular beam epitaxy," Jpn. J. Appl. Phys. **49**(4), 04DH06 (2010).
12. K. C. Shen, W. Y. Lin, D. S. Wuu, S. Y. Huang, K. S. Wen, S. F. Pai, L. W. Wu, and R. H. Horng, "An 83% enhancement in the external quantum efficiency of ultraviolet flip-chip light-emitting diodes with the incorporation of a self-textured oxide mask," IEEE Electron Device Lett. **34**(2), 274–276 (2013).
13. R. H. Horng, K. C. Shen, Y. W. Kuo, and D. S. Wuu, "GaN light emitting diodes with wing-type imbedded contacts," Opt. Express **21**(S1 Suppl 1), A1–A6 (2013).
14. C. Xiong, F. Jiang, W. Fang, L. Wang, C. Mo, and H. Liu, "The characteristics of GaN-based blue LED on Si substrate," J. Lumin. **122–123**, 185–187 (2007).
15. T. Boles, C. Varmazis, D. Carlson, T. Palacios, G. W. Turner, and R. J. Molnar, "High voltage GaN-on-silicon HEMT," Phys. Status Solidi **10**(5), 844–848 (2013).
16. N. Ikeda, Y. Niiyama, H. Kambayashi, Y. Sato, T. Nomura, S. Kato, and S. Yoshida, "GaN Power Transistors on Si Substrates for Switching Applications," Proc. IEEE **98**(7), 1151–1161 (2010).
17. K. C. Shen, T. Y. Wang, D. S. Wuu, and R. H. Horng, "High indium content InGaN films grown by pulsed laser deposition using a dual-compositing target," Opt. Express **20**(14), 15149–15156 (2012).
18. K. C. Shen, T. Y. Wang, D. S. Wuu, and R. H. Horng, "High thermal stability of high indium content InGaN films grown by pulsed laser deposition," Opt. Express **20**(19), 21173–21180 (2012).
19. J. Narayan, P. Pant, W. Wei, R. J. Narayan, and J. D. Budai, "Nanostructured GaN Nucleation Layer for Light-Emitting Diodes," J. Nanosci. Nanotechnol. **7**(8), 2719–2725 (2007).
20. B. Yang, A. Trampert, O. Brandt, B. Jenichen, and K. H. Ploog, "Structural properties of GaN layers on Si(001) grown by plasma-assisted molecular beam epitaxy," J. Appl. Phys. **83**(7), 3800–3806 (1998).
21. T. N. Bhat, M. K. Rajpalke, B. Roul, M. Kumar, and S. B. Krupanidhi, "Substrate nitridation induced modulations in transport properties of wurtzite GaN/p-Si(100) heterojunctions grown by molecular beam epitaxy," J. Appl. Phys. **110**(9), 093718 (2011).
22. K. C. Shen, D. S. Wuu, C. C. Shen, S. L. Ou, and R. H. Horng, "Surface modification on wet-etched patterned sapphire substrates using plasma treatments for improved GaN crystal quality and LED performance," J. Electrochem. Soc. **158**(10), H988–H993 (2011).
23. I. Petrov, P. B. Barna, L. Hultman, and J. E. Greene, "Microstructural evolution during film growth," J. Vac. Sci. Technol. A **21**(5), S117–S128 (2003).
24. Y. Honda, M. Okano, M. Yamaguchi, and N. Sawaki, "Uniform growth of GaN on AlN templated (111)Si substrate by HVPE," Phys. Status Solidi C **2**(7), 2225–2178 (2005).
25. H. Ishikawa, K. Yamamoto, T. Egawa, T. Soga, T. Jimbo, and M. Umeno, "Thermal stability of GaN on (111) Si substrate," J. Cryst. Growth **189–190**, 178–182 (1998).
26. O. H. Nam, M. D. Bremser, T. S. Zheleva, and R. F. Davis, "Lateral epitaxy of low defect density GaN layers via organometallic vapor phase epitaxy," Appl. Phys. Lett. **71**(18), 2638–2640 (1997).
27. Y. Isobe, D. Iida, T. Sakakibara, M. Iwaya, T. Takeuchi, S. Kamiyama, I. Akasaki, H. Amano, M. Imade, Y. Kitaoka, and Y. Mori, "Optimization of initial MOVPE growth of non-polar m- and a-plane GaN on Na flux grown LPE-GaN substrates," Phys. Status Solidi C **8**(7–8), 2095–2097 (2011).
28. M. Hao, H. Ishikawa, and T. Egawa, "Formation chemistry of high density nanocraters on the surface of sapphire substrates with an in situ etching and growth mechanism of device-quality GaN films on the etched substrates," Appl. Phys. Lett. **84**(20), 4041–4043 (2004).
29. J. P. Wilcoxon, G. A. Samara, and P. N. Provencio, "Optical and electronic properties of Si nanoclusters synthesized in inverse micelles," Phys. Rev. B **60**(4), 2704–2714 (1999).
30. T. Takagahara and K. Takeda, "Theory of the quantum confinement effect on excitons in quantum dots of indirect-gap materials," Phys. Rev. B Condens. Matter **46**(23), 15578–15581 (1992).
31. A. L. Patterson, "The Scherrer Formula for X-Ray Particle Size Determination," Phys. Rev. **56**(10), 978–982 (1939).

1. Introduction

GaN-on-Si has recently attracted much interest as an alternative to the GaN-on-sapphire structures used in light-emitting diodes (LEDs) [1–3] and high electron mobility transistors (HEMTs) [4,5] due to the low cost and large production scale of the Si substrate, and its high thermal and electrical conductivity. However, the lattice and thermal mismatches between GaN and Si are as large as 16.7% and 113%, indicating that stress control is required to avoid cracking of GaN on Si, especially when the thickness of the epitaxial GaN layer exceeds 1 μm. Several studies of the strain release in GaN-on-Si growth have proposed using various buffer layer structures (such as an Al_2O_3, AlGaN, AlN/AlGaN superlattice, or SiN_x interlayer) [6–9] and patterned Si substrates [10,11]. Unfortunately, the growth of thicker GaN films (> 2 μm) on Si without crack formation still remains a challenge.

#194888 - $15.00 USD Received 30 Jul 2013; revised 6 Oct 2013; accepted 21 Oct 2013; published 28 Oct 2013

Moreover, for GaN-on-sapphire LEDs, the LED structures are usually designed for and fabricated into different configurations (flip-chip or vertical-type) [12,13] via metal bonding and removal of the sapphire substrate, so as to improve the heat dissipation of the LED and obtain greater power output. A similar approach has been carried out with GaN-on-Si [14]. Generally, GaN is grown on Si(111) substrates due to the three-fold symmetry of this plane, which is a good match to the hexagonal GaN crystallite. However, removal of the Si(111) substrate is not easy because of the difference in bonding energy between Si(111) and Si(100) atoms, resulting in a 20 times slower etching rate of Si(111) (~12 μm/hour for KOH solution at 90°C) than of Si(100). The long substrate removal process degrades the crystal quality and the optoelectronic performance of GaN-on-Si(111) LEDs. On the other hand, for GaN-on-Si HEMTs, although ultrahigh breakdown voltages for GaN power devices on Si(111) have been demonstrated [15,16], integration of GaN HEMTs with advanced Si electronics is difficult, as the Si(100) substrate is more widely used in silicon devices. Therefore, whether LED for enhancing light output or HEMT for integrating Si device, the development of the GaN-on-Si(100) growth is necessary. To this end, we employed high-temperature pulsed laser deposition (PLD) to fabricate a hexagonal GaN template on Si(100). The GaN-on-Si(100) template allows the regrowth of GaN devices without any interlayer through the use of metalorganic chemical vapor deposition (MOCVD). The characteristics of the GaN-on-Si(100) template growth mechanism, crystal quality and optical properties were thoroughly investigated by double-crystal X-ray diffraction (XRD), scanning electron microscopy (SEM), transmission electron microcopy (TEM), atomic force microscopy (AFM), and photoluminescence (PL) measurements.

2. Experimental

All PLD-grown GaN films were grown on a 430 μm-thick Si(100) substrate at 1000°C in nitrogen plasma ambient atmosphere. The working pressure was 1.13×10^{-4} Torr with the injection of N_2 plasma. A KrF excimer laser (λ = 248nm) was employed as the ablation source, and was operated with a repetition rate of 1 Hz and a pulse energy of 60 mJ. The GaN target was fabricated via hydride vapor phase epitaxy and set at a fixed distance of 9 cm from the substrate, and was rotated at 30 rpm during film deposition. We monitored deposition thickness as a function of time in order to understand the growth mechanism of the GaN film on the Si(100) substrate.

3. Results and discussion

Figure 1 shows the XRD pattern of the GaN-on-Si(100) template with a symmetric (002) plane and asymmetric (102) plane. GaN peaks were found at 34.5° and 72.9° for the (002) and (004) plane respectively, as shown in Fig. 1(a), which clearly indicates that hexagonal-GaN (h-GaN) was deposited on the Si(100) by the PLD. A small peak at 69.2°, corresponding to the Si(400) plane, is displayed in the inset of Fig. 1(a). The low peak intensity of this feature was attributed to the limited penetration depth of the X-rays, as the GaN film approached a thickness of 3.54 μm. Similarly, the wurtzite-type GaN peak of the (102) plane is shown in Fig. 1(b). Notably, no cubic-GaN (c-GaN) peak was observed in the XRD pattern, despite the four-fold symmetry of Si(100) being preferred for the growth of a cubic phase. The suppression of c-GaN formation was ascribed to the growth principle of PLD and N_2 plasma nitridation. PLD is a highly nonequilibrium evaporation process, where the stoichiometry of the deposited film is very closely matched to that of the target used [17,18]. In our case, the laser pulse impacted the PLD target and generated GaN vapor, which then reacted with the N_2 plasma and formed GaN on the Si(100). Following the PLD target, the majority of the deposited GaN was thus in the hexagonal phase. Even if some c-GaN had been created by the GaN vapor and N_2 plasma, it would have readily transformed to h-GaN via the formation of stacking faults during depositing [19]. Simultaneously, some N_2 plasma reacted with Si to form Si_xN_y alloys on the surface of Si, and these can disrupt the cubic conformation on Si [20,21]. These factors thus explain why only

#194888 - $15.00 USD Received 30 Jul 2013; revised 6 Oct 2013; accepted 21 Oct 2013; published 28 Oct 2013
(C) 2013 OSA

h-GaN was deposited on the Si(100) substrate. Details pertaining to the growth mechanism are discussed below with reference to SEM and TEM data (see Figs. 2 and 3).

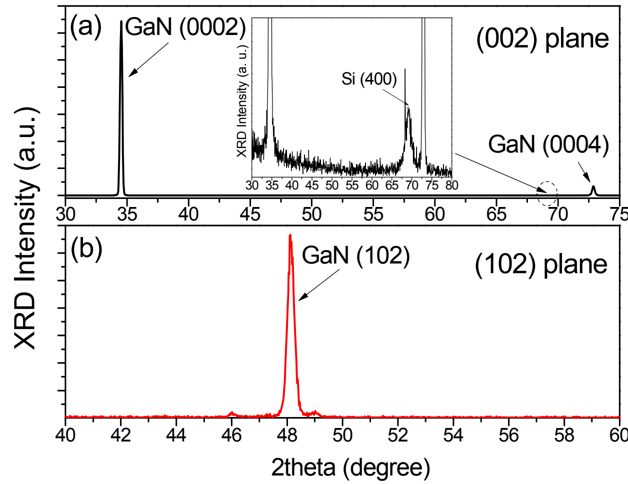

Fig. 1. XRD of GaN-on-Si(100) template at (a) symmetric (002) and (b) asymmetric (102) plane. Inset of Fig. 1(a) shows the peak of the Si(400) plane at 69.2°.

The evolution of the h-GaN growth mode on Si(100) with growth times of 10 min, and 1, 2, and 5 hours is shown in Fig. 2. In Fig. 2(a), one can see that a 210 nm-thick GaN film with grain sizes of 50–80 nm was deposited on the Si(100), which clearly indicated that the beginning of the initial stage of the GaN-on-Si(100) growth is similar to nucleation growth [22,23]. Moreover, since the nitridation process promoted the Si_xN_y formation and prohibited c-GaN nucleation deposition, nucleation of only h-GaN occurred on the surface of Si(100) during the initial deposition. In Figs. 2(b)–2(d), the h-GaN grains started to meet through lateral growth as the growth time increased to 2 hours. After 5 hours of growth, full coalescence generated a relatively smooth surface. The root-mean-squared (RMS) roughness value of the GaN-on-Si(100) was measured by AFM to be 13 nm. The four dashed lines in Fig. 2(e) correspond to the position of the surface morphology shown in Figs. 2(a)–2(d). With increasing growth time, the growth rate of GaN decreased from 1.26 to 0.53 μm/hour, evidenced that the growth mode had completely changed from island (or column) growth to layer growth.

In addition, for common GaN-on-Si growth by MOCVD, high thermal stability AlN (or AlGaN) is usually inserted between GaN and the Si substrate to avoid the occurrence of Ga-Si meltback etching, whereby the Si substrate reacts with Ga decomposed from the GaN grown at low temperature, creating a Ga-Si material during a subsequent rise in temperature [24,25]. This generates large voids on the GaN surface. In contrast, GaN-on-Si growth by PLD will prevent the meltback etching of Ga-Si due to its high-temperature operation.

#194888 - $15.00 USD Received 30 Jul 2013; revised 6 Oct 2013; accepted 21 Oct 2013; published 28 Oct 2013
(C) 2013 OSA

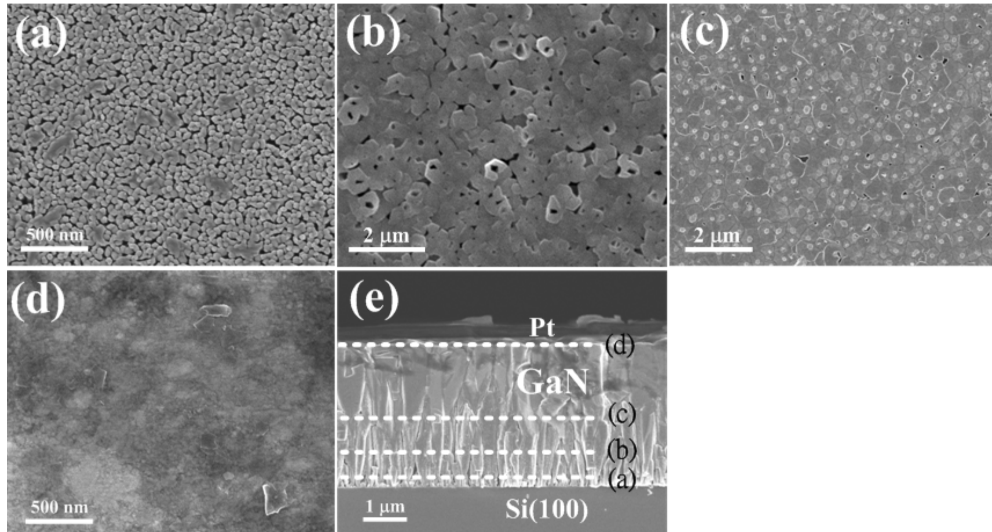

Fig. 2. Surface morphologies of the GaN film deposited on Si(100) substrate after (a) 10 min, and (b) 1, (c) 2, and (d) 5 hours. The four dashed lines in Fig. 2(e) correspond to the position of the surface morphology shown in Figs. 2(a)–2(d).

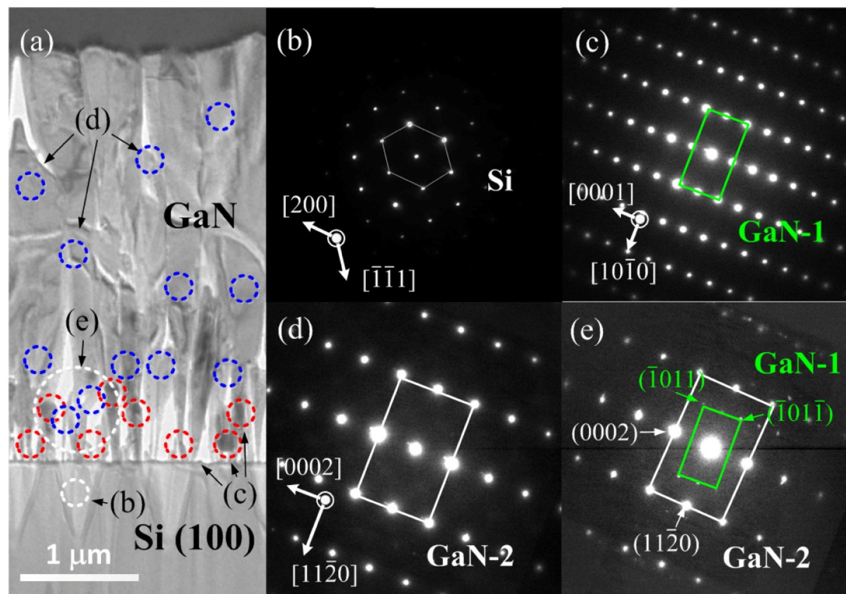

Fig. 3. (a) TEM image of GaN on Si(100) substrate. Electron diffraction patterns of (b) Si, (c) GaN-1, (d) GaN-2, and (e) mixed GaN-1 and GaN-2.

TEM study of the GaN-on-Si(100) template was employed to better understand the nature of the deposited GaN crystals, as illustrated in Fig. 3. Electron diffraction patterns of the circled areas in the cross-sectional TEM image (Fig. 3(a)) are shown in Figs. 3(b)–3(e), which contain two kinds of GaN diffraction patterns as well as that of Si. The first GaN pattern is denoted GaN-1 (marked by the red circle) and the other one is denoted GaN-2 (blue circle). The diffraction pattern of Si captured along the [011] zone axis was considered by the lengths and the angles of the Si patterns. The reciprocal lattice constants of the two types of GaN were measured to calculate the d-spacing. The d-spacing of GaN-1 in the [0001] and [10,10] directions were 0.518 and 0.280 nm respectively. Similarly, for GaN-2, a d-spacing of 0.259

and 0.161 nm along the [0002] and [11–20] directions was verified. The values of the d-spacing are close to the lattice constant of h-GaN. It is notable that the structure of GaN-1 rotated by 90° round the [0002] direction is equivalent to that of GaN-2. It can be inferred that the interaction between the diffusion energy of GaN and the surface energy of Si_xN_y formed by nitridation influenced the arrangement of the h-GaN grains, resulting in two main types of h-GaN depositions. While the GaN-1 was found near the Si surface, the amount of GaN-1 gradually diminished with increasing GaN thickness. GaN-2 formation dominated as the thickness exceeded 1 μm. This was attributed to the lateral growth rate of GaN-2 in the [11–20] direction being faster than that of GaN-1 in the [10,10] direction, resembling to the lateral overgrowth of stripe patterns by MOCVD [26,27]. The lateral growth rate of GaN by PLD is sensitive to the surface roughness and the orientation of facet. To sum up the growth process, a schematic of the growth of GaN-on-Si(100) by PLD is displayed in Fig. 4, illustrating the contribution of PLD and nitridation to induce h-GaN nucleation and facilitating further h-GaN film growth. The growth mode gradually transitions from island growth to layer growth with increasing deposition time.

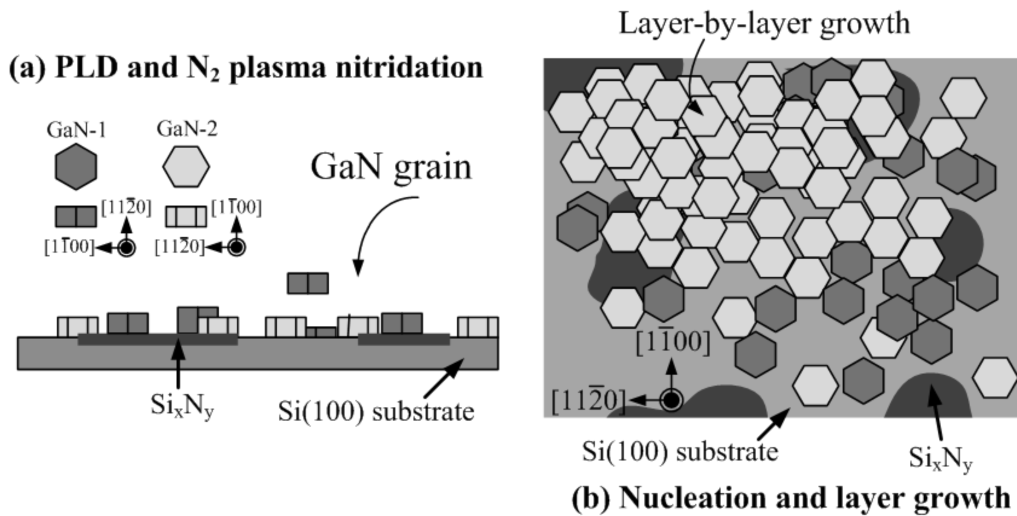

Fig. 4. Schematic illustration for the GaN deposition behavior on Si(100) substrate by PLD (a) cross-view (b) plan-view.

MOCVD was carried out on the GaN-on-Si(100) template to regrow a GaN layer and demonstrate the template reliability. To avoid etching of the PLD GaN film by hydrogen introduced during the regrowth process [28], a 160 nm-thick protected GaN layer was first grown by MOCVD on the template at 950°C in nitrogen ambient atmosphere for 20 min, and a 100 nm-thick un-doped GaN layer was then grown at 1050°C in hydrogen for 10 min. Figure 5 shows the PL spectra of the template before (sample A_1, A_2 and A_5; with subscript 1 denoting deposition by PLD for 1 hour) and after GaN MOCVD regrowth (sample regrowth-A_5). It was found that the peak PL profile of the templates is stronger and sharper with increasing total growth time, and it is accompanied by a shift in peak position from 360 to 365 nm. The peak broadening of the sample A_1 was attributed to the different grain size distribution [29]. Due to the initial island growth of PLD-GaN, as the total growth time increased, the grain size became gradually large, corresponding to a narrower emission of PL spectra. Moreover, the PL peak shift was also explained by a power-law which depended to the crystallite size [30]. The slightly PL red-shift could be considered to the improved GaN crystal quality after MOCVD growth. Additionally, the crystal quality of PLD-GaN film was proven in the XRD rocking curve (in inset of Fig. 5), the full-width half-maximum (FWHM) of (0002) peak of the sample regrowth-A_5 was smaller than of other samples. The decrease of FWHM in XRD profile

#194888 - $15.00 USD Received 30 Jul 2013; revised 6 Oct 2013; accepted 21 Oct 2013; published 28 Oct 2013
(C) 2013 OSA

represented an increase of GaN grain size according to Scherrer formula [31]. Based on the PL and XRD results, they clearly show the reliability of the GaN-on-Si template, and the promising of the GaN-on-Si by PLD for the MOCVD applications.

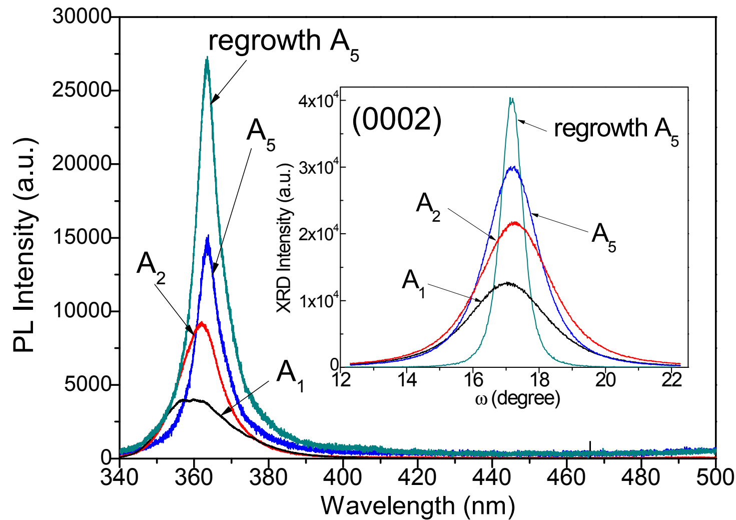

Fig. 5. PL spectra of GaN on Si(100) substrate as a function of growth time. The XRD rocking curve of GaN film before and after MOCVD growth as a function of growth time displayed in the inset of Fig. 5.

4. Conclusion

In conclusion, the growth mechanism and crystal quality of the GaN-on-Si(100) template was verified through the measurement of structural and optical characteristics. During PLD deposition, nitridation influences the nucleation of h-GaN and changes the surface energy of Si(100), leading to mixed h-GaN island growth. The growth mode of GaN-on-Si(100) gradually changes from island growth to layer growth as the growth time exceeds 2 hours. As a proof of concept, the GaN-on-Si(100) template was treated by MOCVD to regrow the GaN layer. The results are clearly promising for MOCVD application using the GaN-on-Si(100) template prepared by PLD.

Acknowledgments

The authors would like to thank the National Science Council of the Republic of China, Taiwan, NSC 101-2221-E-005-023-MY3 and 102-2221-E-005-072-MY3.